ACCURATE INTERATOMIC POTENTIALS FOR Ni, Al AND Ni_3Al

ARTHUR F. VOTER AND SHAO PING CHEN
Theoretical Division, Los Alamos National Laboratory, Los Alamos, NM 87545

ABSTRACT

To obtain meaningful results from atomistic simulations of materials, the interatomic potentials must be capable of reproducing the thermodynamic properties of the system of interest. Pairwise potentials have known deficiencies that make them unsuitable for quantitative investigations of defective regions such as crack tips and free surfaces. Daw and Baskes [Phys. Rev. B **29**, 6443 (1984)] have shown that including a local "volume" term for each atom gives the necessary many-body character without the severe computational dependence of explicit n-body potential terms. Using a similar approach, we have fit an interatomic potential to the Ni_3Al alloy system. This potential can treat diatomic Ni_2, diatomic Al_2, fcc Ni, fcc Al and $L1_2$ Ni_3Al on an equal footing. Details of the fitting procedure are presented, along with the calculation of some properties not included in the fit.

INTRODUCTION

Computer-driven atomistic simulation methods are playing an increasingly important role in the investigation of the structure and properties of materials. Since the usefulness of the results often depends directly on the quality of the interatomic potential employed in the simulation, the development of accurate potentials is of considerable interest.

For metallic systems, the traditional approach has been to use pairwise potentials, either fitted empirically to bulk thermodynamic data [1,2], or derived from pseudopotentials [3]. A simple pair potential has known deficiencies [e.g., the unrelaxed vacancy formation energy is the same as the cohesive energy, and the Cauchy pressure (c_{12}-c_{44}) is zero--neither of these conditions hold true in real solids], which can be remedied by the addition of an energy term that depends explicitly on the volume of the system. The physical basis of this volume dependent term is attributable to the background electron gas in which the ions are embedded. The electron density that each ion senses is dependent on the volume of the crystal. However, this approach is implemented by deriving (or fitting) a pair potential for a particular volume, so that simulations are valid only for a particular density of the system; deviations from this density require a different pair potential. This type of potential is acceptable if the density fluctuations in the simulation are small, but it is clearly inappropriate for defects such as vacancy clusters, crack tips, or free surfaces, since the different atoms sense very different "volumes." This presents a problem, since many important physical processes take place in these defective regions.

A practical solution to this problem has recently been presented by Daw and Baskes [4]. They proposed writing the energy of the system as a pairwise potential plus a term for each atom (the "embedding energy") that is a function of the local electron density that the atom senses due to nearby atoms. Simulation results using these potentials show dramatic improvement over pair potentials [5], with only about twice the computational effort. In essence, the embedding energy provides a local "volume" term for each atom, so that large variations in local atom density can be described accurately.

Using an approach similar to the embedded atom method, potentials have been fit to a number of fcc metals [6]. The approach differs from previous methods primarily in the use of an attractive pairwise interaction and the incorporation of properties of the diatomic molecule in the empirical fit. We present here a potential for the $L1_2$ ordered alloy Ni_3Al, consisting of potentials for fcc Ni and Al, along with an appropriate Ni-Al cross potential. These potentials have been used to simulate grain boundaries [7] and relaxed surface structures [8]. The purpose of the present paper is to present the details of the fitting procedure. The fitting procedure for the pure metals is described in more depth elsewhere [6]. Potentials for Ni_3Al have also been presented by Foiles and Daw [9] and by Eridon, Rehn and Was [10].

Mat. Res. Soc. Symp. Proc. Vol. 82. ©1987 Materials Research Society

THEORY

Homonuclear Systems - Ni and Al

In the embedded atom approach, the energy of an n-particle homonuclear system is written as

$$E = \frac{1}{2}\sum_{\substack{i,j \\ (i\neq j)}}^{n} \phi(r_{ij}) + \sum_{i}^{n} F(\bar{\rho}_i) \quad , \tag{1}$$

where r_{ij} is the distance between atoms i and j, ϕ is a pairwise interaction potential, F is the embedding function, and $\bar{\rho}_i$ is the density at atom i due to all its neighbors,

$$\bar{\rho}_i = \sum_{j(\neq i)}^{n} \rho(r_{ij}) \quad . \tag{2}$$

To mimic the classical electrostatic interaction between two spherical atomic charge densities, the pairwise potential is taken to be a Morse potential,

$$\phi(r) = D_M\{1-\exp[-\alpha_M(r-R_M)]\}^2 - D_M \quad . \tag{3}$$

The three parameters, D_M, R_M, and α_M, define the depth, distance to the minimum, and a measure of the curvature near the minimum, respectively. The density function, $\rho(r)$, is taken as

$$\rho(r) = r^6[e^{-\beta r} + 2^9 e^{-2\beta r}] \quad , \tag{4}$$

where β is an adjustable parameter. This is the density (ignoring normalization) of a hydrogenic 4s orbital, with the second term added to ensure that $\rho(r)$ decreases monotonically with r over the whole range of possible interaction distances (2^9 is the relative normalization factor for a 4s orbital with a doubled exponent). This was chosen for describing first row transition metals, but was found to work well for a number of fcc metals.

Rose et al. [9] have shown that the cohesive energy of most metals can be scaled to a simple universal function, which is approximately

$$E_U(a^*) = -E_0(1+a^*)e^{-a^*} \quad , \tag{5}$$

where a^* is a reduced distance variable and E_0 is the depth of the function at the minimum ($a^*=0$). Following Foiles et al. [5,12], $F(\bar{\rho})$ is specified by requiring that the energy of the fcc crystal obeys Eq. (5) as the lattice constant is varied. The appropriate scaling is obtained by taking E_0 as the equilibrium cohesive energy of the solid (E_{coh}), and defining a^* by

$$a^* = (a/a_0 - 1) / (E_{coh}/9B\Omega)^{1/2} \quad , \tag{6}$$

where a is the lattice constant, a_0 is the equilibrium lattice constant, B is the bulk modulus, and Ω is the equilibrium atomic volume. Thus, knowing E_{coh}, a_0, and B, the embedding function is defined by requiring that the crystal energy from Eq. (5) match the energy from Eq. (1) for all values of a^*. By fitting $F(\bar{\rho})$ in this way, the potential is appropriate for a large range of densities. Note that because a^* cannot be expressed neatly as a function of $\bar{\rho}$, the construction of $F(\bar{\rho})$ is performed numerically once $\phi(r)$ and $\rho(r)$ are known.

To be suitable for use in molecular dynamics and molecular statics simulations, the interatomic potential, and its first derivatives with respect to nuclear coordinates, should be continuous at all geometries of the system. This is accomplished by forcing $\phi(r)$, $\phi'(r)$, $\rho(r)$, and $\rho'(r)$ to go smoothly to zero at a cutoff distance, r_{cut}, which is used as a parameter in the fitting procedure. So that $F(\bar{\rho})$ is properly defined, $E_U(a^*)$ is also modified to go smoothly to zero when the expanded crystal has a nearest neighbor distance equal to r_{cut}.

Having specified the functional forms for $\phi(r)$, $\rho(r)$, and $F(\bar{\rho})$, we now describe the fitting procedure. Because of the way $F(\bar{\rho})$ is determined, the potential always gives a perfect fit to the experimental values of a_o, E_{coh}, and B for any choice of $\phi(r)$ and $\rho(r)$. The remaining five parameters, R_M, D_M, α_M, β, and r_{cut}, are determined by minimizing the root-mean-square deviation (χ_{rms}) between the calculated and experimental values for the three cubic elastic constants (C_{11}, C_{12}, and C_{44}), the vacancy formation energy (ΔE^f_{1v}), and the bond length (R_e) and bond energy (D_e) of the diatomic molecule, and by requiring that the hcp and bcc crystal structures be less stable than fcc. This is accomplished using a simplex search procedure [13].

Including diatomic data in the fit for condensed phase potentials may seem inappropriate. However, good experimental results for diatomics are usually available, enhancing the total amount of experimental data guiding the fit. Since the embedded atom potential should be capable of describing a wide range of atomic densities, the diatomic molecule provides an experimental reference for an environment with very low density. The resulting potential should be more reliable for treating small metal clusters, and processes that generate clusters, such as surface sputtering.

Table I shows the experimental data used in the fits for the two metals, along with the calculated values and χ_{rms}. The fits are seen to be quite good. Allowing the power of r in $\rho(r)$ to vary from 6 [see Eq. (4)], as would be appropriate to describe an Al 3s or 3p orbital density rather than 4s, gave negligible improvement in the fit for Al.

TABLE I. Metal properties used in fit. Calculated values of a_o, E_{coh} and B match experiment exactly due to the way $F(\bar{\rho})$ is determined. Superscripts are the experimental references (a=Ref. 14, b=Ref. 15, c=Ref. 16, d=Ref. 17, e=Ref. 18, f=Ref. 19, g=ref. 20, h=Ref. 21).

Property	Ni		Al	
	expt.	calc.	expt.	calc.
a_o(Å)	3.52[a]		4.05[a]	
E_{coh}(eV)	4.45[b]		3.36[c]	
B (10^{12}erg/cm^3)	1.81[d]		0.79[d]	
C_{11}(10^{12}erg/cm^3)	2.47[d]	2.44	1.14[d]	1.07
C_{12}(10^{12}erg/cm^3)	1.47[d]	1.49	0.619[d]	0.652
C_{44}(10^{12}erg/cm^3)	1.25[d]	1.26	0.316[d]	0.322
ΔE^f_{1v} (eV)	1.60[e]	1.60	0.75[f]	0.73
D_e (eV)	1.95[g]	1.94	1.60[h]	1.54
R_e (Å)	2.2[g]	2.23	2.47[h]	2.45
χ (rms%)	0.75		3.85	

Alloys - Ni_3Al

For a general alloy system, the energy expression becomes

$$E = \frac{1}{2}\sum_{\substack{i,j \\ (i\neq j)}}^{n} \phi_{t_i,t_j}(r_{ij}) + \sum_{i}^{n} F_{t_i}(\bar{\rho}_i) \quad , \quad \bar{\rho}_i = \sum_{j(\neq i)}^{n} \rho_{t_j}(r_{ij}) \tag{7}$$

where the subscripts t_i and t_j indicate atom types. For the binary Ni-Al alloy, the functions ϕ_{NiNi}, ϕ_{NiAl}, ϕ_{AlAl}, ρ_{Ni}, ρ_{Al}, F_{Ni} and F_{Al} are needed. All of these except ϕ_{NiAl} are known from the pure metal fits.

In addition to varying the parameters in ϕ_{NiAl}, two features of the energy expression can be exploited to aid in fitting the alloy properties. Inspection of Eq. (1) shows that the energy of

pure Al is invariant with respect to scaling of ρ_{Al}, if $F_{Al}(\bar{\rho})$ is modified correspondingly; i.e.,

$$\rho_{Al}(r) \longrightarrow s_{Al}\,\rho_{Al}(r) \tag{8}$$

$$F_{Al}(\bar{\rho}) \longrightarrow F_{Al}(\bar{\rho}/s_{Al}) \ . \tag{9}$$

The energy of the alloy system, however, is not invariant with respect to this transformation, so that s_{Al} can be optimized in the alloy fit without affecting the single component potentials. Since the alloy energy is unchanged if both ρ_{Ni} and ρ_{Al} are scaled by the same amount, there is no need for the corresponding parameter, s_{Ni}. Equation (1) is also invariant to the addition of a linear term to $F(\bar{\rho})$,

$$F_{Ni}(\bar{\rho}) \longrightarrow F_{Ni}(\bar{\rho}) + g_{Ni}\bar{\rho}\,, \tag{10}$$

if $\phi(r)$ is transformed as

$$\phi_{NiNi}(r) \longrightarrow \phi_{NiNi}(r) - 2g_{Ni}\rho_{Ni}(r)\ , \tag{11}$$

giving two more parameters (g_{Ni} and g_{Al}) that can be optimized in the fit to alloy properties.

Assuming a Morse potential with variable cutoff distance for $\phi_{NiAl}(r)$, there are a total of seven parameters (D_M, R_M, α_M, r_{cut}, s_{Ni}, g_{Ni}, and g_{Al}) to be optimized in the fit to alloy properties. The experimental quantities used in the simplex fit are the Ni_3Al lattice constant, cohesive energy, elastic constants, ordering energy (ΔE_{ord}), vacancy formation energy, (111) and (100) antiphase boundary (APB) energies, the super intrinsic stacking fault (SISF) energy, and the lattice constant and cohesive energy of B2 phase NiAl (CsCl structure). The subjectively "best" fit, shown in Table II, was achieved by allowing different fitting strengths for the different experimental quantities. The optimized parameters are shown in Table III. The inclusion of the APB and SISF energies was found to be quite important, as neglecting them often led to potentials with negative APB or SISF energies (indicating that the $L1_2$ structure is not the most stable). The data on B2 NiAl was included to broaden the range of stoichiometries over which the potential is valid. The overall potential is thus capable of describing diatomic Ni_2, diatomic Al_2, fcc Ni, fcc Al and $L1_2$ Ni_3Al, and should give a reasonable description of the phases and structures intermediate to these.

DISCUSSION

Figure 1 shows all the functions for the Ni, Al and Ni_3Al potentials. Transformations (8)-(11) leave the potential qualitatively unchanged; the embedding function F provides the repulsion that balances the attractive pairwise potential. For the pure metals, the position of the minimum in $\phi(r)$ is similar to, but less than, the diatomic bond length. While the depth of $\phi_{NiAl}(r)$ lies between $\phi_{NiNi}(r)$ and $\phi_{AlAl}(r)$, the total attraction of Ni for Al is actually stronger than that of Ni for Ni or Al for Al. This is evidenced by the strong diatomic bond in NiAl (calculated to be 2.09 eV), and the stability of the $L1_2$ ordered alloy (which is dominated by Ni-Al nearest-neighbor interactions) relative to the disordered or phase separated alloy.

The best measure of the quality of these potentials can be obtained from an examination of properties not included in the empirical fit. For the pure metals, we calculate a vacancy migration barrier of 0.97 eV for Ni and 0.30 eV for Al, compared to experimental values of 1.3 eV [27] and 0.65 eV [28], respectively. The calculated twin defect energies are 31 mJ/m^2 and 41 mJ/m^2 for Ni and Al, respectively, compared to experimental values of 43±7 mJ/m^2 and 75±11 mJ/m^2 [29]. Surface energies for low index faces of pure Ni fall in the range of 1624 mJ/m^2 [Ni(111) surface] to 2082 mJ/m^2 [Ni(210)], in good agreement with the experimental value for an *average* surface energy of 2280±350 mJ/m^2 [29]. For Al, the corresponding values are 824 mJ/m^2 for (111), 1000 mJ/m^2 for (210), and the experimental value is 980±150 mJ/m^2 [29].

Results are presented elsewhere on the calculated surface relaxations of Ni, Al, Ni_3Al and NiAl [8]. These simulations properly reproduce the qualitative features known experimentally, such as contraction of the first interlayer spacing, oscillations in the deviations of the subsequent interlayer spacings, rippling of mixed-type layers in the alloys (layers containing both Ni and Al), and the outward motion of Al relative to Ni for top layers that are mixed-type.

TABLE II. Metal properties used to fit the Ni_3Al cross potential. Superscripts are the experimental references (a=Ref. 22, b=Ref. 23, c=Ref. 24, d=Ref. 25, e=Ref. 26 f=Ref. 14).

Ni_3Al properties	expt.	calc.
a_0(Å)	3.567[a]	3.573
E_{coh}(eV)	4.57[b]	4.59
$C_{11}(10^{12}erg/cm^3)$	2.30[c]	2.46
$C_{12}(10^{12}erg/cm^3)$	1.50[c]	1.37
$C_{44}(10^{12}erg/cm^3)$	1.31[c]	1.23
ΔE^f_{1v} (eV)	1.6±0.2[d]	1.64(Ni), 1.87(Al)
SISF(111) (mJ/m^2)	10±5[e]	13
APB(100) (mJ/m^2)	140±14[e]	83
APB(111) (mJ/m^2)	180±30[e]	142
B2 NiAl properties		
a_0(Å)	2.88[f]	2.87
E_{coh}(eV)	4.51[b]	4.38

TABLE III. Potential parameters optimized from the fits to experimental data.

	Ni	Al	Ni-Al	
D_M(eV)	1.5335	3.7760	3.0322	s_{Al} = 0.61723
R_M(Å)	2.2053	2.1176	2.0896	g_{Ni} = 6.5145 eV Å^3
α_M(Å^{-1})	1.7728	1.4859	1.6277	g_{Al} = −0.2205 eV Å^3
r_{cut}(Å)	4.7895	5.5550	5.4639	
β(Å^{-1})	3.6408	3.3232		

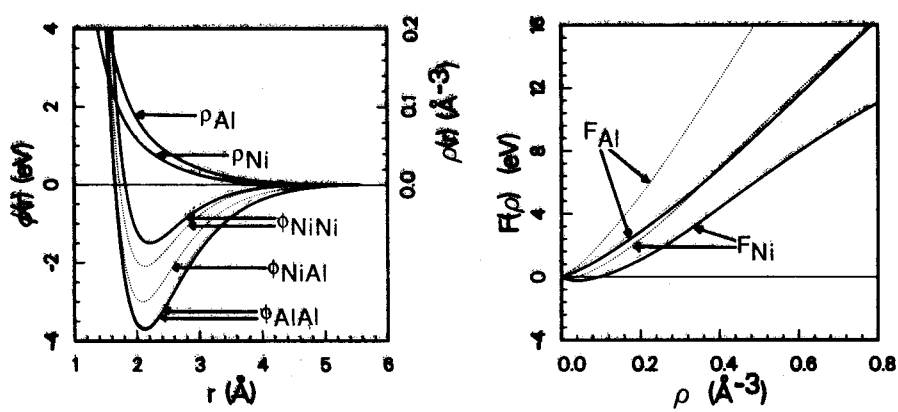

FIG. 1. The functions comprising the Ni_3Al potential. The ρ_{Al} curve has been scaled by s_{Al}. Where two curves are displayed, the dotted line represents the function after the transformations of Eqs. (8)-(11).

Quantitative comparisons with the experimental data (from, e.g., low energy electron diffraction) on changes in interlayer spacings show agreement within a factor of two. Simulations of Ni_3Al grain boundaries using these potentials [7] show that Al-rich grain boundaries have the highest energy, consistent with experimental data on the stoichiometry effects on the mechanical properties of Ni_3Al.

ACKNOWLEDGMENTS

The authors are grateful to S. M. Foiles, M. S. Daw and M. I. Baskes for communication of unpublished work, and to D. J. Srolovitz, D. Farkas and P. J. Hay for helpful discussions. This work was supported by the Energy Conversion and Utilization Technologies (ECUT) Program of the U. S. Department of Energy.

REFERENCES

[1] R.A. Johnson and W. D. Wilson, in Interatomic Potentials and Simulation of Lattice Defects, edited by P.C. Gehlen, J.R. Beeler, and R.I. Jaffee (Plenum, New York, 1971).
[2] T. Halichioglu and G.M. Pound, Phys. Status Solidi A 30, 619 (1975).
[3] W.A. Harrison, Pseudopotentials in the Theory of Metals (Benjamin, New York, 1966).
[4] M.S. Daw and M.I. Baskes, Phys. Rev B 29, 6443 (1984).
[5] S.M. Foiles, M.I. Baskes and M.S. Daw, Phys. Rev. B 33, 7983 (1986), and references therein.
[6] A.F. Voter, to be published.
[7] S.P. Chen, A.F. Voter and D.J. Srolovitz, Scripta Met. 20, 1389 (1986); Proceedings of the 1986 Materials Research Society Conference, Boston, 1986, Symposium H.
[8] S.P. Chen, A.F. Voter, and D.J. Srolovitz, Phys. Rev. Lett., 57, 1308 (1986); S.P. Chen, A.F. Voter and D. J .Srolovitz, these proceedings, page___.
[9] S. M. Foiles and M. S. Daw, J. Mater. Res., in press.
[10] J. Eridon, L. Rehn and G. Was, in press for publication in Nucl. Instr. Methods B, April 1987.
[11] J.H. Rose, J.R. Smith, F. Guinea and J. Ferrante, Phys. Rev. B 29, 2963 (1984).
[12] S.M. Foiles, Phys. Rev. B 32, 7685 (1985).
[13] J.A. Nelder and R. Mead, Comp. J. 7, 308 (1965).
[14] C. Kittel, Introduction to Solid State Physics, 5th ed. (Wiley, New York, 1976).
[15] Metal Reference Book, 5th ed., edited by C.J. Smith (Butterworths, London, 1976).
[16] Handbook of Chemistry and Physics, edited by R.C. Weast (CRC, Boca Raton, FL, 1984).
[17] G. Simons and H. Wang, Single Crystal Elastic Constants and Calculated Aggregate Properties (MIT Press, Cambridge, Massachusetts, 1977).
[18] R. W. Ballufi, J. Nucl. Materials 69, 240 (1978).
[19] J.S. Koehler, in Vacancies and Interstitials in Metals, edited by A. Seeger, D. Schumacher, W. Schilling and J. Diehl (North Holland, Amsterdam, 1970), p. 175.
[20] J.O. Noell, M.D. Newton, P.J. Hay, R.L. Martin, and F.W. Bobrowicz, J. Chem. Phys. 73, 2360 (1980).
[21] K.P. Huber and G. Hertzberg, Constants of Diatomic Molecules (Van Nostrand Reinhold, New York, 1979).
[22] S. Stassis, Phys. Stat. Socl. A 64, 335 (1981).
[23] R. Hultgren, P.D. Desai, D.T. Hawkins, M. Gleiser, and K.K. Kelley, Selected Values of the Thermodynamic Properties of Binary Alloys (ASM, Metals Park, Ohio, 1973).
[24] M.H. Yoo, privatae communication. Values from Ref. 20 were scaled to T = OK according to values in K. Ono and R. Stern, Trans. AIME **245**, 171 (1969).
[25] T.-M. Wang, M. Shimotomai, and M. Doyama, J. Phys. F 14, 37 (1984).
[26] P. Veyssiere, J. Douin, and P. Beauchamp. Phil. Mag. A 51, 469 (1985).
[27] W. Wycisk and M. Feller-Kniepmeier, J. Nuc. Mater. **69&70**, 616 (1978).
[28] W. Schule and R. Scholz, in Point Defects and Defect Interactions in Metals, edited by J. -I. Takamura, M. Doyama and M. Kiritani (University of Tokyo Press/North Holland, Amsterdam, 1982), p257.
[29] L. E. Murr, Interfacial Phenomena in Metals and Alloys (Addison Wesley, Reading, MA, 1975).